APPLIED PHYSICS LETTERS **92**, 101112 (2008)

Monte Carlo study of GaN versus GaAs terahertz quantum cascade structures

Enrico Bellotti, Kristina Driscoll, Theodore D. Moustakas, and Roberto Paiella[a)]
Department of Electrical and Computer Engineering and Photonics Center, Boston University, 8 Saint Mary's Street, Boston, Massachusetts 02215, USA

(Received 19 December 2007; accepted 18 February 2008; published online 11 March 2008)

Due to their large optical phonon energies, nitride semiconductors are promising for the development of terahertz quantum cascade lasers with dramatically improved high-temperature performance relative to existing GaAs devices. Here, we present a rigorous Monte Carlo study of carrier dynamics in two structures based on the same design scheme for emission at 2 THz, consisting of GaN/AlGaN or GaAs/AlGaAs quantum wells. The population inversion and hence the gain coefficient of the nitride device are found to exhibit a much weaker (by a factor of over 3) temperature dependence and to remain large enough for laser action even without cryogenic cooling. © *2008 American Institute of Physics*. [DOI: 10.1063/1.2894508]

Technological development in the terahertz spectral region has so far been limited, as conventional device concepts from both the electrical and the optical domain cannot be readily extended to operation at terahertz frequencies. Yet, the potential of terahertz radiation in numerous fields, including medical diagnostics, security screening, and manufacturing quality control, has recently been identified and is driving extensive research efforts to develop the required components. In the area of terahertz sources, a promising approach is provided by the quantum cascade (QC) laser scheme based on intersubband (ISB) transitions in semiconductor quantum wells (QWs). In this lasing modality, the emission wavelength is tailored through the design of the multiple-QW active material and thus can be tuned by design over a broad spectral range. Terahertz QC lasers based on GaAs/AlGaAs QWs have, in fact, been developed in the past few years and currently span the 1.2–5 THz range with peak output powers often on the order of a few tens milliwatts.[1–5]

Although these advancements are impressive, the operation of GaAs/AlGaAs terahertz QC lasers fundamentally requires cryogenic cooling, with maximum temperatures reported so far near 170 and 120 K for pulsed and continuous-wave emission, respectively.[2] This important limitation is related to an intrinsic property of the GaAs/AlGaAs material system, namely, the presence of longitudinal optical (LO) phonons with energies $h\nu_{\mathrm{LO}}$ relatively close to the room-temperature thermal energy k_BT of 26 meV (e.g., $h\nu_{\mathrm{LO}}=36$ meV in GaAs). As a result, laser action at or near room temperature is precluded by the process of thermally activated LO-phonon emission. This nonradiative decay mechanism is illustrated schematically in Fig. 1, where the traces labeled $|u\rangle$ and $|l\rangle$ denote the upper and lower laser subbands, respectively. At cryogenic temperatures, a large population inversion can be established since the majority of electrons in $|u\rangle$ occupy states near the bottom of the subband, from which they cannot decay nonradiatively into $|l\rangle$ via LO-phonon emission because of the requirement of energy conservation. As the temperature is increased, however, more and more electrons in $|u\rangle$ can gain enough thermal energy that scattering into $|l\rangle$ via LO-phonon emission becomes allowed. Since these scattering processes are ultrafast, the end result is a dramatic reduction in the device population inversion and optical gain. A recent experimental study has concluded that this mechanism is indeed the main factor limiting the maximum operating temperature of GaAs/AlGaAs terahertz QC lasers.[3]

This argument suggests the exploration of novel semiconductor heterostructures having larger LO-phonon frequencies as a means to improve the high-temperature performance of terahertz injection lasers. One promising system currently attracting considerable attention for various applications of ISB transitions is that of GaN/AlGaN QWs, where the LO-phonon energies lie in the 91–99 meV range. As a result, in a GaN-based terahertz QC laser, the breakdown in device performance due to the onset of thermally activated LO-phonon emission can be expected to occur at much higher temperatures. Previous theoretical studies, based on rate-equation models of varying complexity, have suggested that even room-temperature terahertz lasing may be feasible with III-nitride QWs.[6,7] The goal of this work is to provide a rigorous comparison between GaAs/AlGaAs and GaN/AlGaN terahertz QC structures where both material systems are treated on equal footing, in order to properly quantify the potential for improvement offered by the latter system.

To that purpose, we employ a microscopic model of carrier dynamics in QC gain media based on a set of Boltzmann-like equations solved with a Monte Carlo technique.[8–11] Unlike rate-equation models (even those including carrier-carrier scattering), this approach allows us to fully take into account the presence of nonequilibrium carrier distributions in QC gain media and their effect on the ISB scattering rates. This is particularly important in the description of terahertz QC lasers, where electron-electron scattering (which strongly depends on the global carrier distribution) plays a prominent role in determining the population inversion. Additionally, in order to obtain the fairest possible comparison between the two material systems under consideration, we have carried out simulations of two QC structures based on the same design scheme[5] and with the same target emission frequency of 2 THz (8.2 meV), one consist-

[a)]Electronic mail: rpaiella@bu.edu.

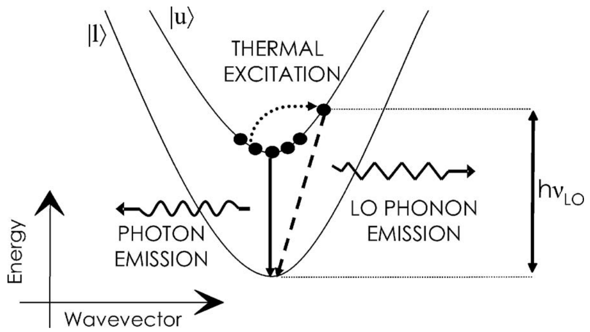

FIG. 1. Schematic illustration of the competition between photon emission and thermally activated LO-phonon emission by electrons in the upper laser subband of a terahertz QC structure.

ing of $GaN/Al_{0.15}Ga_{0.85}N$ QWs, and the other of $GaAs/Al_{0.15}Ga_{0.85}As$ QWs.

The two QC gain media were designed using a Schrödinger-equation solver based on the effective-mass approximation, with the characteristic built-in electric fields of nitride heterostructures included explicitly.[12] Shown in Figs. 2(a) and 2(b) are the conduction-band profiles and squared envelope functions of the relevant bound states of the GaN and GaAs structures, respectively, under optimal bias conditions. The optical transitions occur between the states labeled $|4\rangle$ and $|3\rangle$ in each period of these active materials. The lower laser states are rapidly depopulated through tunneling into state $|2\rangle$ downstream and scattering into state $|1\rangle$ via resonant LO-phonon emission. To maximize the speed of the latter process, in both structures, the energy separation between subbands $|1\rangle$ and $|2\rangle$ is close to the LO-phonon energy of the well material. This QC design scheme has been successfully demonstrated in a recent GaAs/AlGaAs device[5] and was chosen for this study because of its inherent simplicity as it contains only three QWs per repeat unit. In the GaN structure, the intrinsic piezoelectric fields were computed assuming an $Al_{0.07}Ga_{0.93}N$ strain-balancing growth template. It should be noted that GaN wells and $Al_{0.15}Ga_{0.85}N$ barriers grown on such template are under relatively low strain (-0.19% and 0.22%, respectively). The corresponding theoretical and experimental critical thicknesses for plastic relaxation are on the order of at least several hundred angstroms,[13] well above the layer thicknesses used in the GaN structure of Fig. 2(a) (listed in the caption). Therefore, strain relaxation will not be a limiting factor in the growth of high-quality gain media consisting of many repetitions of this QC design.

In our simulations, a particle-based Monte Carlo approach is used to determine the steady-state carrier distributions of the laser subbands as a function of temperature, starting from a constant population initially assigned to each subband. The numerical model includes four subbands per period, and a total of three adjacent periods is simulated. Periodic boundary conditions are applied such that for each particle exiting the third repeat unit, a new one is injected in the first. Electron/electron and electron/LO-phonon scattering are both included in the simulations,[14] with the relevant scattering rates at a given temperature computed and stored for each subband pair for a discrete number of initial electron energies. During the Monte Carlo simulation, an interpolation is used to determine the rates at arbitrary initial energy values. The electron final state after scattering with a LO phonon is determined using a rejection technique on the scattering angle probability distribution,[15] which is precomputed as a function of the electron initial energy, stored, and used as a two-dimensional look-up table. The final state after an electron/electron scattering event is obtained using a multiple-rejection approach, and the relevant probability distribution is generated using the four-subband overlap integrals.[10] Particularly critical is the treatment of screening,[16,17] and in this work we employ a temperature dependent single-subband screening approach.

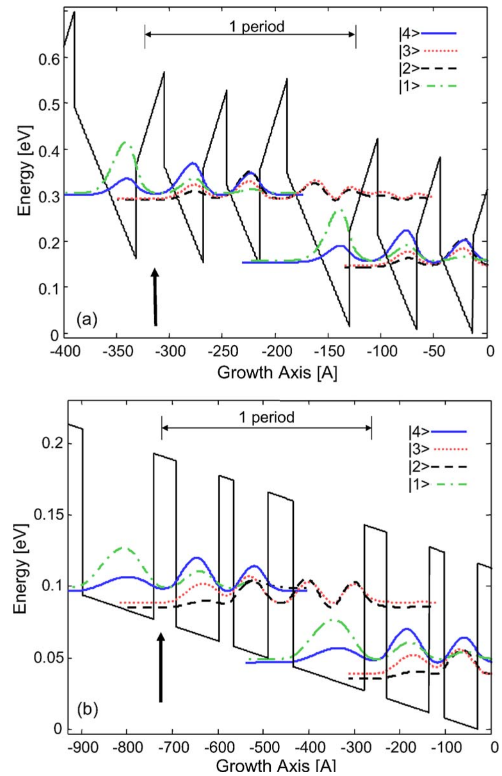

FIG. 2. (Color online) Conduction-band profile and squared envelope functions of (a) the $GaN/Al_{0.15}Ga_{0.85}N$ and (b) the $GaAs/Al_{0.15}Ga_{0.85}As$ QC gain media considered in this study. The two structures are plotted in the presence of an external field of (a) 73 kV/cm and (b) 11 kV/cm. The layer thicknesses of a single stage, starting from the injection barrier (indicated by the arrow) and moving downstream, are **26**/37/**22**/31/**26**/59 Å for the GaN structure and **49**/94/**33**/74/**56**/156 Å for the GaAs structure (the boldfaced numbers refer to the barrier layers).

In Fig. 3, we plot the calculated fractional population inversion $\Delta n \equiv (n_4 - n_3)/n_{tot}$ versus temperature for the two

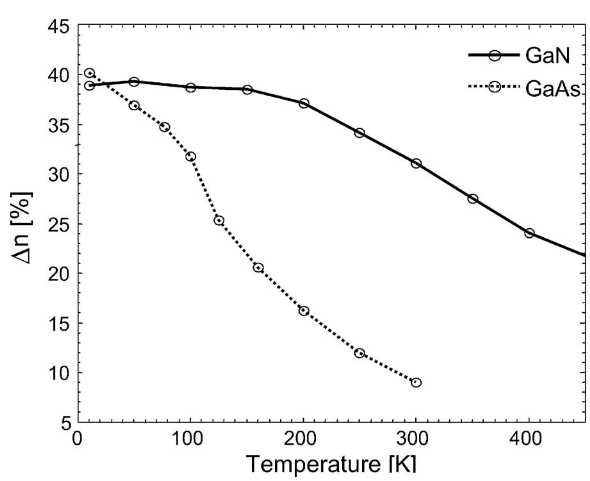

FIG. 3. Calculated fractional population inversion of the terahertz QC structures of Fig. 2(a) (solid line) and Fig. 2(b) (dotted line) vs temperature.

structures of Figs. 2(a) and 2(b). Here, n_4 and n_3 are the sheet electron densities of the upper and lower laser subbands, respectively, and n_{tot} is the total electron density per period, taken to be 2×10^{10} cm^{-2}. The results shown in this figure fully support and quantify the claim that GaN terahertz QC gain media can provide better performance compared to GaAs devices. In particular, Δn in the GaN structure is found to degrade much more slowly with increasing temperature compared to the GaAs device. For example, as the temperature is increased from 10 to 300 K, Δn in the GaN structure decreases only by a factor of 1.25 versus 4.48 in the GaAs gain medium. These numerical results are consistent with the severe performance degradation with increasing temperature experimentally observed in GaAs terahertz QC lasers, which is caused by thermally activated LO-phonon emission and (to a lesser extent[3]) by thermal backfilling of the lower laser states $|3\rangle$ from the states $|1\rangle$ downstream. Both of these limiting factors are much less effective in the presence of the large LO-phonon energies of nitride QWs, as clearly indicated by our simulation results.

The maximum operating temperature of the two gain media can be estimated from the plots of Fig. 3 as the temperature beyond which Δn is smaller than the population inversion required to reach laser threshold. In QC lasers, the latter quantity can be written as follows:[18]

$$\Delta n_{\mathrm{th}} = \frac{1}{n_{\mathrm{tot}}}\frac{\alpha\varepsilon_o \eta c \gamma L_p}{\Gamma N_p \omega q^2 z^2}, \quad (1)$$

where η is the refractive index, γ the full width at half maximum of the gain spectrum, L_p the length of one period of the active material, Γ the optical confinement factor per period, N_p the number of periods, $\hbar\omega$ is the energy of the emitted photons, α the total cavity loss coefficient, and qz the electric dipole moment of the laser transition. From our simulations shown in Figs. 2(a) and 2(b), we have $L_p=201$ Å and $z=33$ Å for the GaN structure and $L_p=462$ Å and $z=66$ Å for the GaAs structure. For the refractive indices near 2 THz, we use the experimentally determined values of 3 and 3.8 for GaN and GaAs, respectively.[9,19] Furthermore, from previously reported measurements with GaAs terahertz-QC-laser waveguides based on surface plasmons,[2,4] we take $\alpha/\Gamma N_p = 20$ cm^{-1} for both structures.

Regarding the gain linewidth, a typical value for the GaAs device under study extrapolated from the literature is $\gamma\approx 3$ meV.[9] This can be ascribed partly to lifetime broadening (given the ultrafast, ~100 s fs, phonon-assisted depopulation of the lower laser states) and partly to broadening due to surface roughness. Using this value in Eq. (1), we calculate for the GaAs structure of Fig. 2(b) a minimum population inversion required to achieve lasing $\Delta n_{\mathrm{th}}=16.3\%$. The resulting maximum operating temperature obtained from the simulation results of Fig. 3 is $T_{\max}\approx 200$ K. This value is reasonably close to the largest working temperature reported to date with GaAs devices, approximately 170 K,[2] indicating that our model accurately describes the temperature dependent performance of terahertz QC lasers.

If the same linewidth of 3 meV is assumed for the GaN structure of Fig. 2(a), a threshold population inversion of 22.1% and a maximum operating temperature of over 400 K are obtained. Furthermore, the ability of this device to operate without cryogenic cooling (i.e., at temperatures accessible with thermoelectric coolers, >250 K) is predicted for linewidths up to over 4.6 meV. Due to the narrower wells of this GaN design compared to the GaAs structure, interface roughness may be expected to play a larger role in broadening the gain line. On the other hand, the large effective masses and strong built-in electric fields of nitride QWs make their bound-state energies less sensitive to thickness fluctuations than in GaAs wells of similar thickness, as confirmed by Schrödinger-solver-based simulations. Experimentally, while no measurements at terahertz frequencies have yet been reported, near-infrared ISB absorption peaks with large quality factors (e.g., 40 meV linewidth for absorption near 870 meV) have been obtained in narrower (and more highly strained) GaN/AlN QWs.[20] It should also be noted that, in general the interface-roughness-limited quality factor $\hbar\omega/\gamma$ of ISB transitions tends to increase with increasing well width.[21] Thus, nitride terahertz QC structures with the required relatively low ISB linewidths are expected to be feasible. While the growth and experimental demonstration of these devices remain a considerable challenge (mainly due to the present lack of high-quality GaN substrates), the prospect of operation without cryogenic cooling presented here should provide strong impetus for their investigation.

This work was supported by the Army Research Laboratory. Partial support for E. B. has been provided by NSF through Grant No. ECS-0449232.

[1] R. Köhler, A. Tredicucci, F. Beltram, H. E. Beere, E. H. Linfield, A. G. Davies, D. A. Ritchie, R. C. Iotti, and F. Rossi, Nature (London) **417**, 156 (2002).
[2] B. S. Williams, S. Kumar, Q. Hu, and J. L. Reno, Opt. Express **13**, 3331 (2005).
[3] B. S. Williams, S. Kumar, Q. Qin, Q. Hu, and J. L. Reno, Appl. Phys. Lett. **88**, 261101 (2006).
[4] C. Walther, G. Scalari, J. Faist, H. Beere, and D. Ritchie, Appl. Phys. Lett. **89**, 231121 (2006).
[5] H. Luo, S. R. Laframboise, Z. R. Wasilewski, G. C. Aers, H. C. Liu, and J. C. Cao, Appl. Phys. Lett. **90**, 041112 (2007).
[6] V. D. Jovanović, D. Indjin, Z. Ikonić, and P. Harrison, Appl. Phys. Lett. **84**, 2995 (2004).
[7] G. Sun, R. A. Soref, and J. B. Khurgin, Superlattices Microstruct. **37**, 107 (2005).
[8] R. Köhler, R. C. Iotti, A. Tredicucci, and F. Rossi, Appl. Phys. Lett. **79**, 3920 (2001).
[9] H. Callebaut, S. Kumar, B. S. Williams, Q. Hu, and J. L. Reno, Appl. Phys. Lett. **83**, 207 (2003).
[10] O. Bonno, J. L. Thobel, and F. Dessenne, J. Appl. Phys. **97**, 043702 (2005).
[11] C. Jirauschek, G. Scarpa, P. Lugli, M. S. Vitiello, and G. Scamarcio, J. Appl. Phys. **101**, 086109 (2007).
[12] S. Gunna, F. Bertazzi, R. Paiella, and E. Bellotti, in *Nitride Semiconductor Devices: Principles and Simulations*, edited by J. Piprek (Wiley, New York, 2007), Chap. 6.
[13] I. Akasaki and H. Amano, in *Gallium Nitride (GaN) I*, edited by J. I. Pankove and T. D. Moustakas (Academic, New York, 1998), Chap. 15.
[14] M. Mosko and A. Moskova, Phys. Rev. B **44**, 10794 (1991).
[15] S. M. Goodnik and P. Lugli, Phys. Rev. B **37**, 2578 (1988).
[16] J. H. Smet, C. G. Fonstad, and Q. Hu, J. Appl. Phys. **79**, 9305 (1996).
[17] S. C. Lee and I. Galbraith, Phys. Rev. B **59**, 15796 (1999).
[18] C. Sirtori and R. Teissier, in *Intersubband Transitions in Quantum Structures*, edited by R. Paiella (McGraw-Hill, New York, 2006), Chap. 1.
[19] W. Zhang, A. K. Azad, and D. Grischkowsky, Appl. Phys. Lett. **82**, 2841 (2003).
[20] L. Nevou, M. Tchernycheva, L. Doyennette, F. H. Julien, E. Warde, R. Colombelli, F. Guillot, S. Leconte, E. Monroy, T. Remmele, and M. Albrecht, Superlattices Microstruct. **40**, 412 (2006).
[21] M. Helm, in *Intersubband Transitions in Quantum Wells: Physics and Device Applications I*, edited by H. C. Liu and F. Capasso (Academic, New York, 2000), Chap. 1.